

Modelling of the initial failure of CFRP structures by partial discretisation: a micro / macro-mechanical approach of first ply failure

Bodo Fiedler¹, Stefan Holst¹, Thomas Hobbiebrunken², Masaki Hojo², Karl Schulte¹

¹Polymer Composite Section, Technical University Hamburg-Harburg, Germany

²Department of Mechanical Engineering, Graduate School of Engineering, Kyoto University, Japan

The formation of transverse matrix cracks is the early failure in carbon fibre reinforced composites (CFRP). Unidirectional laminates with 90° fibre orientation were tested by transverse tensile tests and in situ under 3 point bending load in the scanning electron microscope (SEM). Finite element analysis were carried on a hexagonal unit cell of fibre and matrix, as on the macroscopic level based on homogenized fibre and matrix properties as well. The link of the micromechanical approach with the homogenized description of composite structures was done by transferring boundary conditions from one model to the other. The influence of the temperature on the Young's modulus, the non-linear stress-strain behaviour and the strength of the matrix on the micro residual stresses and matrix failure was taken into account and investigated in detail.

1. INTRODUCTION

High performance composites based on polymeric matrix are manufactured at elevated temperatures. Shrinkage during curing and the mismatch of the coefficient of thermal expansion (CTE) between fibre and matrix are the most important reasons for residual stresses. For composite systems with a polymer matrix, the fibre has usually a lower coefficient of thermal expansion than the matrix. The residual stresses have a strong effect on the mechanical performance of composites. It is revealed that the presence of residual stresses reduces the transverse strength to failure [1]. When the residual stresses are sufficiently large, microcracks can be induced. Residual stresses can lead to transverse failure, especially in cross ply laminates [2]. The final stress state in the matrix depends on temperature dependent mechanical and thermal properties of fibre and matrix. Especially the matrix properties respond very sensitive to temperature. Young's modulus, yield stress, and CTE may vary over a wide range during cooling from the manufacturing temperature. The temperature dependent non-linear matrix behaviour is one of the most important among them, because matrix plasticity can change the residual stress state predicted from the elastic case. In general, residual stresses are reduced by plastic flow [3]. However, the increase of yield stress and of residual stresses are a competing process and after curing and cooling the composite; the matrix is subjected to a triaxial stress state [3].

When load is applied to the composite, the triaxial stresses in the matrix increase. Both the polymer matrix and the fibres cannot behave as they would individually as neat materials, and the difference in the Poisson's ratios causes a triaxial stress state reducing the maximum bearable load. It was clearly shown that the hydrostatic tensile stress severely reduces strain to failure of an epoxy resin compared to the results of a uniaxial tensile test [4,6]. The authors showed in an earlier work that the parabolic criterion is suitable to describe the experimentally observed macroscopic yield and fracture behaviour of epoxy resins [7].

In commercially applied composites, the fibre distribution is more scattered and the local fibre volume fraction V_{f1} may vary from much less than average volume fraction V_f (resin rich areas) to maximum values (close contact) where resin pockets are formed. Therefore, both effects can occur and both result in local tensile and compressive stresses. Photoelastic studies on multiple fibre square arranged composites showed that the radial stress is about 1.6 times higher than expected from calculations using a simple cylindrical model [8]. Analytical calculations have strong limitations concerning boundary conditions, non-linear material behaviour, large strains

etc. Numerical approaches like FEA are suitable to investigate the residual stresses on the micro mechanical level.

The authors previously [9] studied the residual stresses by finite element analysis and photo elastic analysis with regard to the influence on interfacial contact and analysed the micro-residual stresses by a finite element analysis. Depending on the local fibre distribution, these stresses can improve or reduce the local ultimate transverse strength of the composite [10].

The influence of the local fibre volume fraction on the initial matrix failure and on the interfacial failure consists of two aspects: with increasing local fibre volume fraction, the geometrical influence reduces the stress values of failure and the residual stresses depend on the ratio of local to nominal volume fraction leading to the opposite effect. The calculated strength values show only a slight influence of the thermal residual stresses because the residual stresses and the related geometrical change (fibre distance) of local fibre volume fraction [1] are compensating effects.

The failure behaviour of epoxy resins was studied and discussed in detail [7,11]. Prediction of residual stresses and induced matrix failure requires knowledge of the temperature dependent mechanical and thermal properties of the constituents. The temperature dependent nonlinear matrix behaviour is one of the most important among them, because matrix plasticity lowers the residual stress state predicted for the elastic case.

The state of the art criteria [12,13] to describe the failure of composite structures are based on homogenised properties and they can not regard on the micromechanical level of fibre and matrix. On the micromechanical level many models exist to describe the fracture phenomena observed in composites. High performance composites are cured at higher temperatures, after curing and cooling the composite is subjected to residual stresses. The resulting tri-axial stress state has a strong effect on the mechanical performance of composites. It is revealed that the presence of residual stresses reduce the transverse strength to failure [14].

In the past three decades numerous researchers investigated residual stresses in composite materials by using analytical, numerical and/or experimental approaches. Most analyses regards on thermal expansion mismatch between the constituents [15].

However, analytical calculations have strong limitations concerning boundary conditions, nonlinear material behaviour, large strains etc., the finite element analysis is a suitable method to investigate the residual stresses on the micromechanical level. Fiedler, et al. [9] studied the residual stresses by finite element and photo elastic analysis with regard to the influence on interfacial contact.

However, transferring the results obtained on micromechanical level to the level of composite structures is difficult. The present work regards on this problem. The finite element analysis is used to link the micromechanical approach with the homogenised description of composite structures. Considering as example a 3 point bending specimen made from CFRP (HTA/L135), the results obtained by the modelling are in good agreement compared to the results from in-situ 3 point bending tests carried out in SEM.

2. MATERIALS AND EXPERIMENTS

Carbon fibre reinforced polymer (CFRP) panels were manufactured by resin-transfer-moulding (RTM) with three layers of Hexcel unidirectional (UD) G1157 fabric and MGS L135i/H137 epoxy system as matrix. The RTM is schematically shown in Fig. 1. The G1157 fabric consists by weight of 96% HTA carbon fibres in 0°-direction of the fabric and 4% E-glass fibres in 90°-direction. The low viscose L135i/H137 epoxy resin system is optimised for RTM to be injected and cured at room temperature (RT). To prepare UD samples (ISO 527-4) containing only UD-

carbon fibres the portion of weft glass fibre rovings were removed in sections from the UD plain weave fabric before resin infusion. The operating pressure in the vessel was $P=0.2$ MPa and the supporting vacuum in the trap was less than $P<0.005$ MPa.

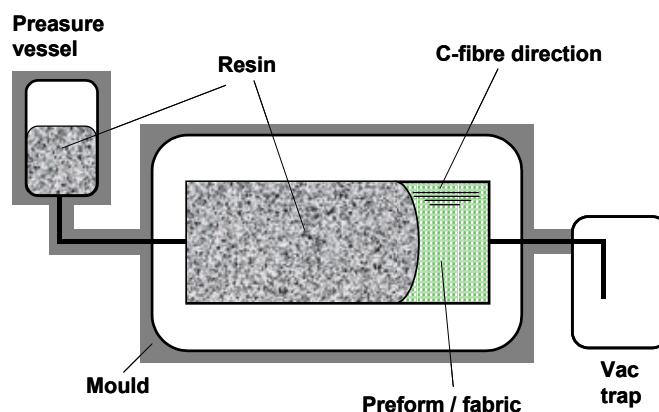


Fig. 1 Laboratory scale RTM.

After curing, the samples for the transverse test were cut from the CFRP panel which had an average thickness of 1.07 ± 0.03 mm and an average fibre volume fraction of 44.3 ± 1.3 %. In case of the 3 point bending test, the specimens were cut from 3 ± 0.05 mm thick panels. All specimens were post cured at 60°C for 24 hours. In Fig. 2 a polished cross section is shown. A homogenous fibre distribution and a void free matrix was achieved.

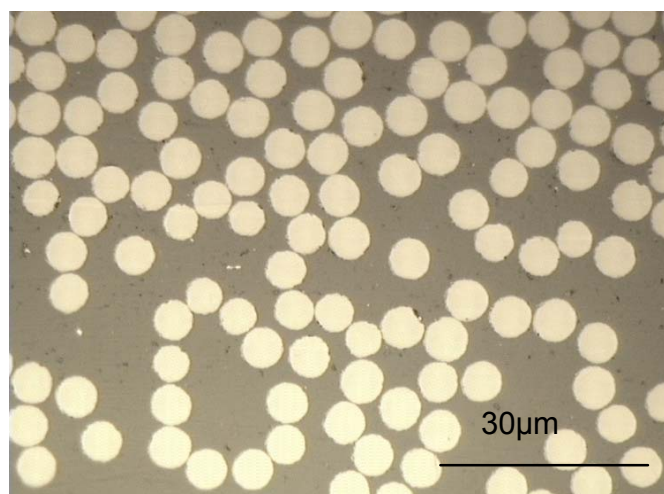


Fig. 2 Polished cross section of L135/HTA composite (light micrograph).

The elastic properties are summarized in Tab. 1 and the thermal properties in Tab. 2, based on experimental results, data sheet values and calculations [16,17]. They are the data basis for carrying out the FEA.

Table 1 Elastic constants of fibre, matrix and composite ($V_f=50\%$).

Cons. [MPa]	Resin L135	Fiber HTA	Composite ($V_f=0.6$)
E_{11}	2900	238000	14400
E_{22}	-	28000	8600
E_{33}	-	28000	8600
G_{12}	1100	50000	2600
G_{23}	-	5000	1900
G_{31}	-	24000	2600
ν_{12}	0.35	0.28	0.28
ν_{23}	-	0.23	0.66
ν_{31}	-	0.02	0.01

Table 2 Coefficients of thermal expansion (CTE) of fibre, matrix and composite ($V_f=50\%$).

CTE	Resin L135	Fiber HTA 5131	Composite HTA ($V_f=60\%$)
α_{11} [$\mu\text{m}/\text{m}\cdot\text{K}$]	50	-0.1	-0.006
α_{22}, α_{33} [$\mu\text{m}/\text{m}\cdot\text{K}$]	50	10	30

3. FINITE ELEMENT ANALYSIS

The method carried out is to read off force or displacements at the critical region of a larger sized composite FE-model, consisting of homogenized properties of fibre and matrix. Transferring these data as new boundary conditions to the discrete or partial discrete FE-model. The partial discrete model is self-contained and the new boundary conditions are applied along the edges (2D analysis) of the model. The approach is illustrated in Fig. 3.

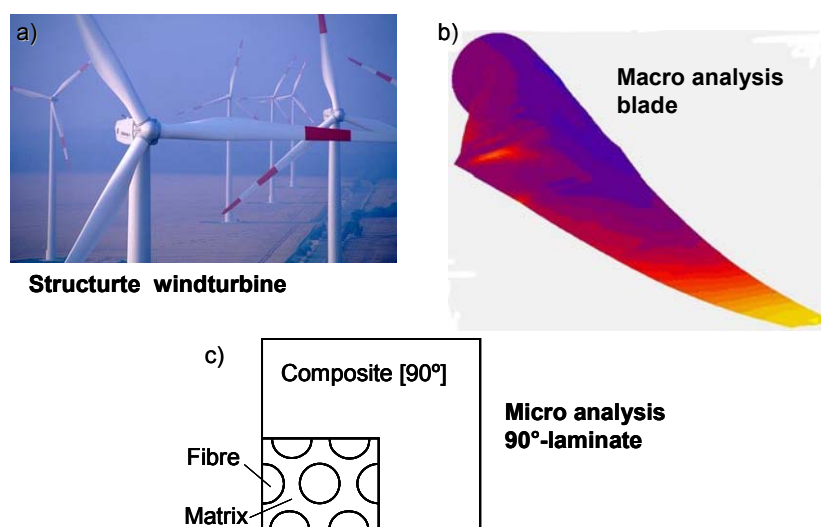


Fig. 3 Multi scale FEA to link macro laminate stress with micro stresses; a) Arneburg Wind Power Facility, Germany - 30 MW [18]; b) Macro FE analysis of spatial distribution of blade longitudinal blade strain; c) Micro FE analysis of [90°] Laminate.

In practice the extraction of the loads in the most critical area of the structure is done by writing the data into an ASCII file. When needed these data are readjusted by interpolation and coordinate transformation to the partial discrete model. The flow chart is shown in Fig. 4.

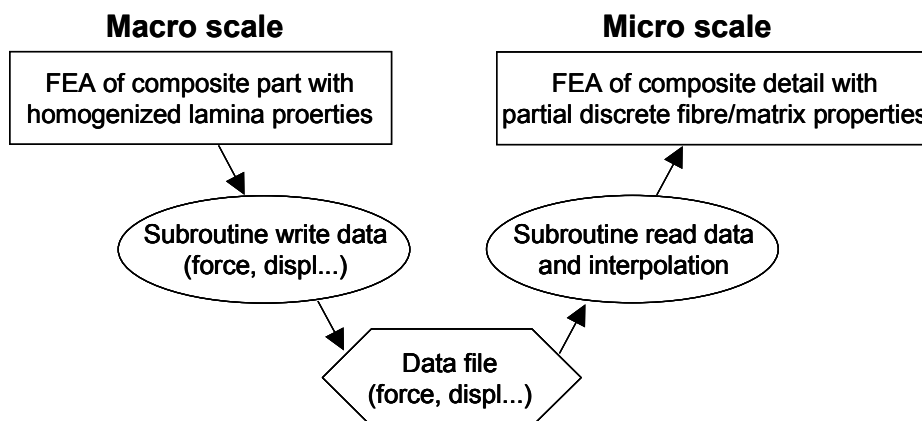


Fig. 4 Method of how to apply the Partial Discretisation and transfer boundary conditions.

The numerical calculations were carried out using the commercial finite element code MARC/Mentat™ (version 2001). The FEA model has been described previously elsewhere [1,11]. The model consists of a microscopic unit cell with matrix and fibres in a hexagonal array and a homogenised area with properties of a unidirectional composite. According to the rule of mixture (ROM) the volume fraction of the discrete part of the model and for the composite elements was constant at $V_f=50\%$. The discrete area is only 0.25% of the entire FE-model, so that the stiffness of the FE-Model is not affected by the variation of the local fibre volume fraction (Fig. 6).

The 2-D FE mesh consists of 4-node plain strain elements. The residual stresses of the matrix were taken from the unit cell around the central fibre in a distance of $0.65\ \mu\text{m}$ from the fibre surface. The mechanical and thermo-mechanical properties of fibres, matrix and composite were incorporated into the FEA model. Fibres and composite were taken as orthotropic materials. Tables incorporate the elastic constants and the thermal-mechanical behaviour of the fibre, matrix and composite elements into the FEA. The epoxy matrix was assumed to be isotropic and the yield criterion is v. Mises criterion. The work-hardening option and the corresponding plastic strain and stress data incorporated the non-linear stress/strain behaviour of the epoxy resin.

4. MODELLING STRESSES ON MACRO SCALE

On the macroscopic scale the bending beam was modelled by a 2 dimensional analysis (2D-FEA). The beam thickness of 3 mm was regarded by the geometric property input of the FE-software. Using the symmetry only one half of the beam is needed (Fig. 5a).

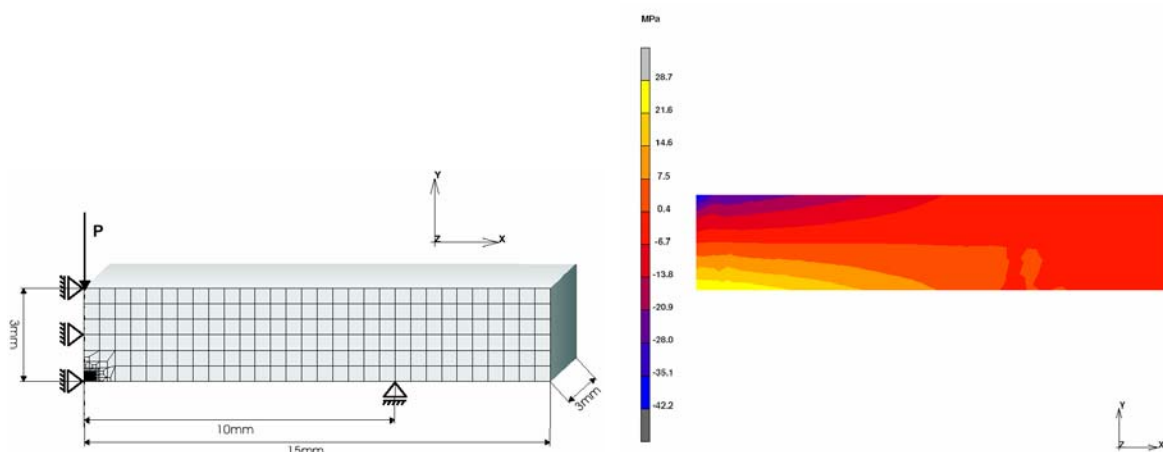


Fig. 5 a) 2D-FE mesh with homogenized $[90^\circ]$ laminate properties of the bending beam. b) Stress distribution in x-direction obtained by the 2D-FEA, applied load is 25.4 N

Fig. 5b illustrates the results obtained from the FEA. It shows the well known tensile stresses at the bottom of the beam tensile stress of $\sigma_x=28.7$ MPa and compressive values at the upper surface. At an applied load of $P=25.4$ N the corresponding maximum tensile stress of $\sigma_x=28.7$ MPa at the surface was calculated, which fits well to the results of the classical laminate theory (CLT) resulting for the same load in a maximum tensile stress of $\sigma_x=25.8$ MPa.

5. PARTIAL DISCRETE MODEL

The partial discrete model is a self consisting model of a $[90^\circ]$ -laminate and is shown in Fig. 6b schematically. The mesh of the discrete part is given in Fig. 6a. At first the micro-residual stresses were calculated by cooling from $T=80^\circ\text{C}$ to RT. After this first step, the bending displacements u were applied as boundary conditions according to Fig. 6b.

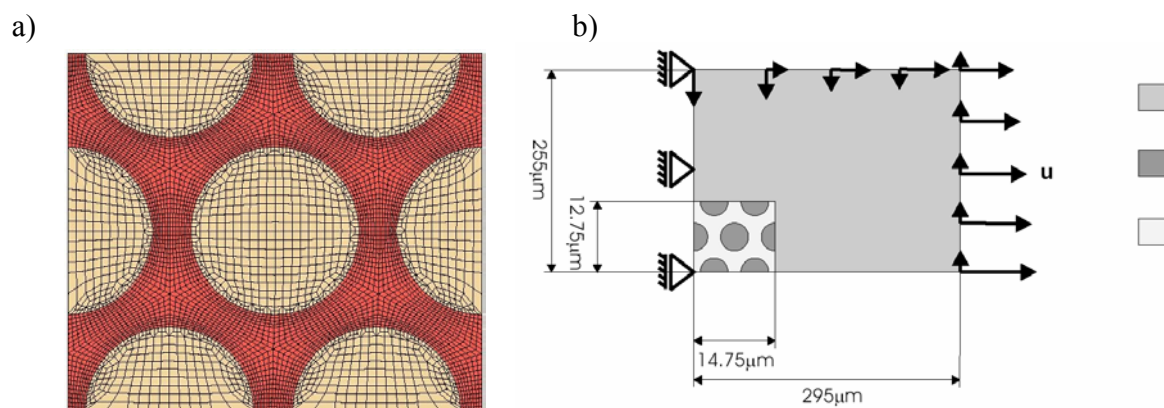


Fig. 6 a) FE mesh of the hexagon unit cell, cut out from the partial discrete model; b) Modelling of local stresses on micro level (schematic).

Fig. 7. illustrates the micro residual radial stress σ_R (a) and the hoop stress σ_H distribution around the centre fibre of the hexagon fibre array. A symmetric stress distribution results from the cooling to RT. The stresses are not constant along the circumference of the centre fibre, the

minimum stress is $\sigma_{Rmin} = -3.5$ MPa and the maximum value $\sigma_{Rmax} = -0.7$ MPa, respectively. In case of the of hoop stress the values are $\sigma_{Hmin} = 8.3$ MPa and $\sigma_{Hmax} = 9.4$ MPa.

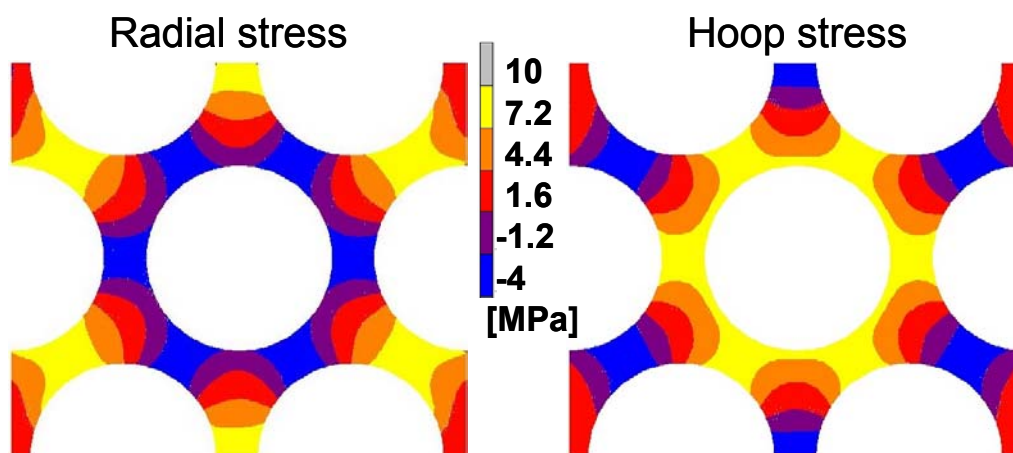


Fig. 7 Micro thermal residual stresses in the matrix; a) Radial stress; b) Hoop stress.

Incremental load steps were read from the data file. The initial failure in the matrix occurred at an applied load of $P=52$ N, which corresponds to a laminate tensile stress in the outer surface of $\sigma_x=45,9$ MPa. Compared to results obtained by calculations of transverse tensile tests the stress values at failure are similar [19]. The location of initial matrix failure is in between the fibres. The failure criterion of the matrix is the parabolic criterion worked out in our former investigations [10,11,14]. Failure occurs when the octahedral shear and normal stress values reach a critical value with regard to the hydrostatic stress state. The spatial distribution of the matrix failure shows Fig. 8, in case the value reaches "1" failure occurs.

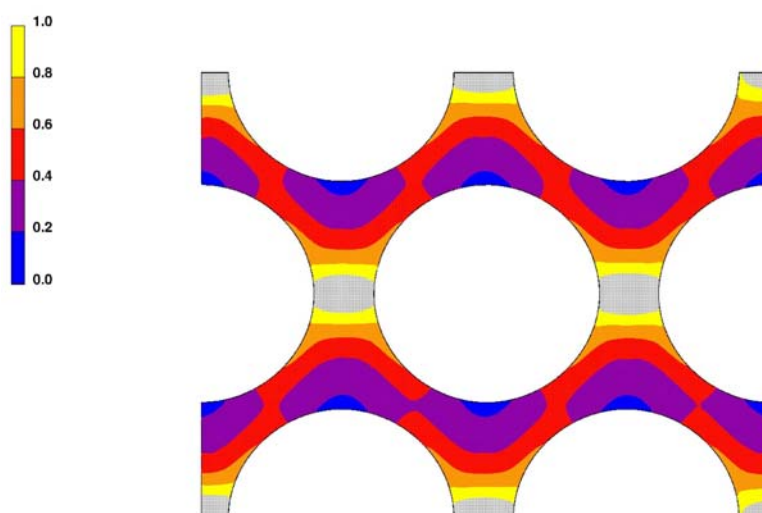


Fig. 8 Spatial distribution of the parabolic failure criterion; only the matrix is shown.

6. IN SITU BENDING TEST IN SEM

The deflection of the beam was applied by a crank handle, the resulting force was measured by load cell. To obtain initial failure the load was applied stepwise. During scanning the area of about 20 mm² a slight drop of the force was measured due to relaxation of the specimen. The side of observation was not sputtered by gold, therefore the non conductive matrix is highlighted (Fig. 9). The fracture of the 3 point bending specimens were brittle and it was extremely difficult to get the picture of initial failure. In one case it was possible to observe initial failure at an applied load of P=56 N (Fig. 9a). Just before final failure (P=104±5 N) of the specimen, Fig. 9b was taken. It shows a rather long crack growth in the specimen.

Taking into account the drop in stress while observing the specimen surface in the SEM, the experimental results are in good agreement with the calculated load for initial failure of the matrix.

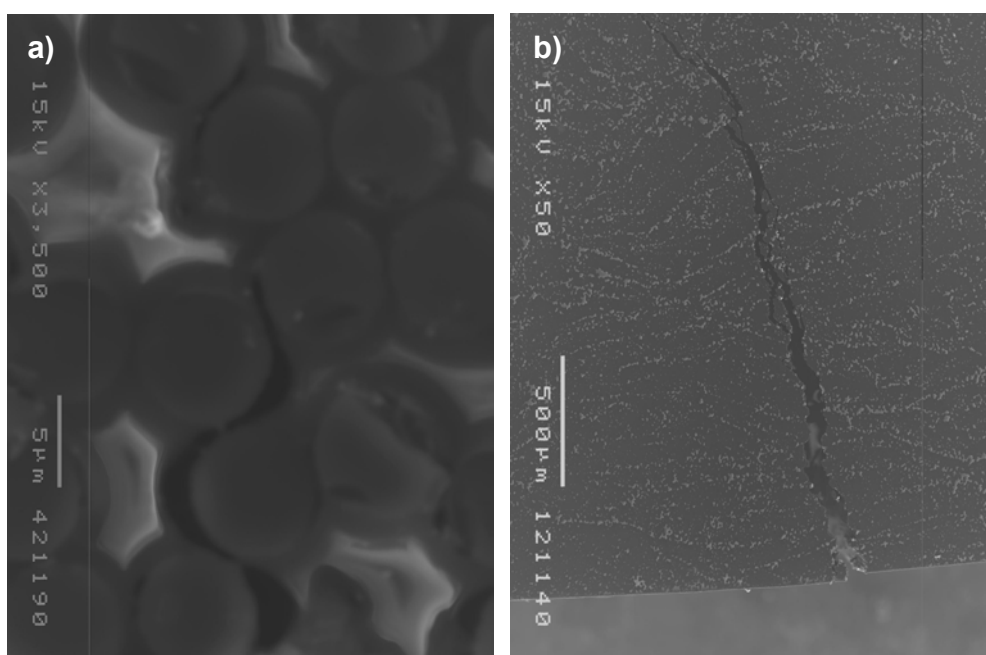


Fig. 9 SEM Micrograph of in situ bending test of L135/HTA 90°-composites; a) Initial failure (P=56 N); b) Just before final failure (P=104 N).

7. CONCLUSIONS

The spatial distribution of thermal residual stresses are not constant in the matrix and are strongly affected by the neighbouring fibres.

Linking micro and macro FEA is possible by using the boundary data transfer approach to the partial discrete model.

It is possible to directly observe initial failure of 3 point bending specimen in SEM. The calculated initial load of failure, regarding the experimental difficulties is in good agreement with the calculated values.

ACKNOWLEDGEMENT

This work was supported in the frame of the collaborative program of the German Research Foundation (DFG) and the Japan Society for Promotion of Science (JSPS) and in the frame of the Center of Excellence (COE) program of the Ministry of Education, Sports, Science and Technology.

References

- 1 **B. Fiedler, M. Hojo, S. Ochiai**, The influence of thermal residual stresses on the transverse strength of CFRP using FEM. *Composites: Part A* 33 (2002), pp. 1323-1326.
- 2 **S. Kobayashi, K. Terada, S. Ogihara, N. Takeda**. Damage-mechanics analysis of matrix cracking in cross-ply CFRP laminates under thermal fatigue. *Composite Science and Technology* 61 (2001), pp.1735-1742.
- 3 **Hull, D. and Clyne, T. W.**, An introduction to composite materials, 2nd edition, edited by Clarke, D. R., Suresh, S., Ward, I. M., Cambridge University Press, (1996).
- 4 **Asp, L. E., Berglund, L. A., Talreja, R.**, Prediction of Matrix-Initiated Transverse Failure in Polymer Composites, *Composite Science and Technology*, 56, (1996), pp. 1089-1097.
- 5 **Asp, L. E., Berglund, L. A.**, Effects of a Composite-Like Stress State on the Fracture of Epoxies, *Composite Science and Technology*, 53, (1995), pp. 127-37.
- 6 **Asp, L. E., Berglund, L. A., Talreja, R.**, A Criterion for Crack Initiation in Glassy Polymers Subjected to a Composite Like Stress State, *Composite Science and Technology*, 56, (1996), pp. 1089-1301.
- 7 **Fiedler, B., Hojo, M., Ochiai, S., Schulte, K., Ando, M.**, Failure behavior of epoxy matrix under different kinds of static loading, *Composites Science and Technology*, 61/11 (2001), pp 1615-1624.
- 8 **Chamis, C., C.**, Mechanics of load transfer at the interface, *Composite Materials*, Vol. 6, pp. 31-77 (Plueddemann, Editor), Academic Press (1974).
- 9 **Fiedler, B., Klisch, A., Schulte, K.**, Thermal residual stresses in fibre reinforced polymers. Proceedings of ACCM-I, Osaka, Japan; October 7-9, (1998). pp. 604-1-604-4.
- 10 **Fiedler, B., Hojo, M., Ochiai, S., Schulte, K., Ochi, M.**, Finite-element modeling of initial matrix failure in CFRP under static transverse tensile load. *Composites Science and Technology* 2001;61:95-105.
- 11 **Fiedler, B., Hojo, M., Ochiai, S.**, The parabolic failure criterion applied to epoxy resins. Proceedings of International Conference on new Challenges in Mesomechanics, Aalborg, Denmark, August 26-30, 2002, 533-539.
- 12 **R. Hill**, The Mathematical Theory of Plasticity, Oxford University Press, London 1950
- 13 **S.W. Tasi, E.M. Wu**, A general theory of strength for anisotropic materials, *J. Comp. Mat.* 1971, 5, 58-80.
- 14 **Fiedler, B., Hojo, M., Ochiai, S.**, The influence of thermal residual stresses on the transverse strength of CFRP using FEM. *Composites: Part A* 33 2002, 1323-1326.
- 15 **J.A. Nairn**, Thermoelastic Analysis of Residual Stresses in Unidirectional, High Performance Composites, *Polymer composites*, (1985), Vol. 2, No. 2, 123-130.
- 16 MARTIN G.SCHEUFLER KUNSTHARZPRODUKTE GMBH: Produkt data sheet resin, L135, curing agent 133-138.
- 17 TENAX FIBRES GMBH : Produkt data sheet HTA6K
- 18 General Electric Company, American Sales Headquarters & Wind Turbine Manufacturing Facility, 13000 Jameson Road, Tehachapi, CA 93561, USA
- 19 **B. Fiedler, A. Gagel, T. Hobbiebrunken, M. Hojo, K. Schulte, S. Ochiai**, Modelling of the thermal residual stresses and the transverse strength of CFRP at low and high temperatures, *Composites Part A*, 2004, special issue from IIMM Balatonfüred, Hungary, submitted